Baligar et al. Int J Stem Cell Res Ther 2016, 3:034
DOI: 10.23937/2469-570X/1410034
Volume 3 | Issue 1

International Journal of
Stem Cell Research & Therapy

ISSN: 2469-570X

Research Article: Open Access

Bone Marrow Cells Repair and Regenerate Acute and Chronic Injured Liver without Primary Evidence of Neoplastic Changes

Prakash Baligar[1,2], Veena Kochat[1], Snehasish Mukherjee[1], Abinaya Sundari T[1], Vikash Kumar[1], Zaffar Equbal[1] and Asok Mukhopadhyay[1]*

[1]*Stem Cell Biology, National Institute of Immunology, New Delhi, India*

[2]*Amity Institute of Molecular Medicine and Stem Cell Research (AIMMSCR), Amity University, Noida, India*

***Corresponding author:** *Asok Mukhopadhyay, PhD, National Institute of Immunology, Aruna Asaf Ali Marg, New Delhi-110067, India, Tel: 91-11-26715004, Fax: 91-11-26742125, E-mail: ashok@nii.ac.in*

Abstract

Therapeutic potential of bone marrow (BM)-derived cells in acute and chronic liver injury model has been investigated. Apart from pathological improvement of the liver, we also studied liver regeneration and genetic alteration in donor cells towards neoplasia. Acetaminophen-induced acute and CCl4-induced chronic liver injured male mice were transplanted with BM-derived uncommitted and $CD45^+$ cells, respectively from female mice. Transplantation of CD45 cells resulted in enhanced recovery of fibrotic liver during initial pro-fibrogenic condition as compared with sham control. Significant recovery from apoptotic death of hepatocytes was also observed. After 3 months of transplantation, donor-derived hepatocytes in acute and chronic liver injury models were found to be about 5% and 17%, respectively. Real-time RT-PCR analyses revealed that neither donor-derived hepatocytes nor recipient liver expressed pluripotency (*Oct4, Nanog, Sox2*) and α-fetoprotein (*AFP*) genes, a suppressive response of tumor-related *Cyclin D2* was also seen. About 96% of the donor-derived hepatocytes were devoid of *Sry* gene and contain only XX chromosome. Thus, BM-derived cells were found to be a potential therapeutic tool for the treatment of both acute and chronic liver diseases. Preliminary results suggested that post nuclear reprogramming of BM cells does not lead to activation of neoplastic genes.

Keywords

Acute liver injury, Liver fibrosis, Bone marrow cells, Liver regeneration, Cellular transformation

Introduction

All major metabolic and synthesis functions of liver are significantly perturbed in case of critical injury. Though liver regenerates by itself following acute injury, this process is impaired in case of chronic injury. In both cases, unless liver is allowed to regenerate by proving appropriate support, either internally or externally, depending up on the extent of injury it ceases to function and transplantation remains the only available treatment option.

Adult BM-derived cells were found to contribute towards liver regeneration in irradiation-induced acute injury model, but due to inadequate selection pressure the involvement of these cells in liver regeneration remains low [1-5]. The first successful report was published in case of fumarylacetoacetate hydrolase knockout ($Fah^{-/-}$) mouse model, in which dietary supplement 2-(2-Nitro-4-trimethylbenzoyl)-1,3-cyclohexadione (NTBC) was used to ameliorate liver damage. The recipient of wild type BM progenitor cells, following withdrawal of NTBC, showed not only phenotype correction, the liver nodules also exhibited 50-70% chimerism with donor-derived cells [6,7]. It was shown than the newly formed hepatocytes, generated from the fused heterokaryons, can expand rapidly owing to a considerable survival advantage in the absence of NTBC [8,9]. Despite inherent limitation of low contribution in liver regeneration, BM-derived cells have been used in many studies involving experimental animals and human subjects [10-12]. All these studies have focused on the feasibility of BM cell therapy to treat diseases like inborn metabolic disorders or liver cirrhosis [6,13-18]. It is not clearly understood whether BM cells are directly involved in regeneration of liver, though the paracrine effect of the same in activation of hepatic progenitor cells (HPCs) has been reported [19]. In this study we have adopted two experimental liver disease models. The rationale for choosing these models was that acute injury model resembles liver damage due to overdose of toxin, whereas chronic injury mimics liver damage due to prolonged inflammatory response. In case of liver failure, whole organ or hepatocytes transplantation has been limited due to global shortage of donor livers; hence an alternative therapeutic approach is warranted. Again, cell fusion leads to polyploidy and chromosomal instability, both considered to be the early events in carcinogenesis. Thus, it is important that the BM-derived hepatocytes be examined for such cellular changes, if any. Here we have addressed the following questions: a) does the phenotype change from hematopoietic to hepatic lineage results in the activation of genes that are associated with neoplastic changes, b) whether the host chromosome is completely segregated from the donor-derived hepatocytes after the cell fusion, and c) in case of chronic injury, can the donor cells also take part in regeneration of liver apart from the resolution of fibrosis.

Materials and Methods

Experimental acute and chronic liver injury model

Acute liver injury model was established by single dose (500 mg/kg body weight) injection of acetaminophen (Tablets India Ltd.,

Citation: Baligar P, Kochat V, Mukherjee S, Abinaya ST, Kumar V, et al. (2016) Bone Marrow Cells Repair and Regenerate Acute and Chronic Injured Liver without Primary Evidence of Neoplastic Changes. Int J Stem Cell Res Ther 3:034. doi.org/10.23937/2469-570X/1410034

Received: April 20, 2016: **Accepted:** May 24, 2016: **Published:** May 28, 2016

ClinMed International Library

Chennai, India) via intraperitoneal route. Chronic liver injury model was established by repeated injection (0.8 ml/kg body weight) of 10% CCl_4 (CDH, Mumbai, India) in mineral oil (Sigma-Aldrich, St. Louise), twice a week, for a period of 10 weeks via intraperitoneal route. Pro-fibrotic condition was maintained by CCl_4 injection (0.4 ml/kg body weight) for 15 days after transplantation of the cells.

The extent of liver injury was assessed by histopathology and sera ALT levels. The measurement of ALT activity was carried out using a commercially available kit (Transasia Bio-medicals Ltd, New Delhi, India). In brief, the rate of NADH oxidation was determined in a coupled reaction employing lactate dehydrogenase (LD). The oxidation of NADH to NAD^+ is accompanied by decrease in absorbance at 340 nm. In the sera samples where ALT is rate limiting, the decrease of absorbance is directly proportional to the activity of ALT. To determine the extent of liver fibrosis, 5-µm sections of formalin fixed liver of different time points, embedded in paraffin, were cut from different lobes (parallel sections were not considered). The sections were stained with hematoxylin (Sigma-Aldrich, Bangalore, India) followed by picrosirius red (Polyscience Inc., Warrington, PA). Finally, the collagen proportionate area (CPA) was measured using ImageJ software (NIH, Bethesda, MD) considering only the stained area. The activation status of HpSCs was examined by staining with α-smooth muscle actin (α-SMA) antibody, followed by determining the α-SMA area as explained above.

Transplantation of cells

Lin- BM cells were isolated from eGFP-expressing female C57Bl/6J mice following negative selection with MACS kit (Miltenyi Biotec, Gladbach, Germany). Two hundred fifty thousand Lin- BM cells were transplanted in each mouse in a group of 12 with acute liver injury through intravenous route and another 6 mice (sham control) received normal saline. For isolation of $CD45^+$ cells, mononuclear BM cells of eGFP transgenic female C57Bl/6J mice were stained with mouse anti-CD45/APC (BD Bioscience) and then sorted using FACS AriaIII (BD Bioscience, CA). Thirty six chronic liver injured mice were divided equally into two groups, sham control (ShC) and transplantation (Tx). ShC mice received normal saline and Tx group received 5 million sorted $CD45^+$ cells through intrasplenic route.

In chronic injury model, the purpose of using high cell dose was for repair (resolution of fibrosis) and liver regeneration; whereas, in case of acute injury low cell dose was used as they were required only for liver regeneration. In fibrotic liver, the collagenous scar is mainly degraded by MMPs secreted from monocytes/macrophages (CD11b) and neutrophils (Ly6g) (~ 55% of $CD45^+$ BM cells). In separate experiments, three more groups of fibrotic mice were used; in the first group (n = 3) each mouse received same cells (CD45) as before, in second group (n = 3) 3 million $CD45^+CD11b^+Ly6g^{+/-}$ cells and in third group (n = 3) of mice 2 million $CD45^+CD11b^-Ly6g^-$ cells were transplanted.

Supporting methods

Other methods, including liver perfusion, isolation of hepatocytes, phenotypic characterization of cells, TUNEL assay, FISH, liver function tests, reverse transcriptase polymerase chain reaction, primer design (Table 1), etc. are described.

Statistics

Results of multiple experiments were reported as mean ± SEM (Standard Error Mean). Student's t-test was carried out to calculate the significance between the means of both groups and p value < 0.05 was considered as significant. All analyses were carried out using Graph pad Prism software, Version 5.02.

Results

Recovery of liver function depends on the nature and the extent of injury

A single dose (500 mg/kg body weight) of acetaminophen led to centrilobular necrosis of the liver, which healed considerably within 4 days (Figure 1A, top panel). These changes in liver pathology were coupled with steep rise in serum ALT levels, which later declined towards the normal level as liver regeneration progressed (Figure 1B). In chronic injury model, gross tissue necrosis was not observed even after 10 weeks of CCl_4 administration, instead putative fibrotic

Table 1: Primers used for qPCR analyses.

Gene	Primer sequence
Gata2	ATGAATGGACAGAACCGGC (forward) TCGTCTGACAATTTGCACAAC (reverse)
CD45	AAGTGCAGAAACAGAAGATG (forward) CGATGATGTCATAGAGGAAC (reverse)
Sca1	AGGAGGGAGCTGCTAGGTTT (forward) CAGTAGGGCCACAAGAAGAATC (reverse)
Oct4	GAGGGAACCTCCTCTGAGCC (forward) GCAGGGCTTTCATGTCCTGG (reverse)
Sox2	ATGAACGGCTCGCCCACCTA (forward) CTGGAGCTGGCCTCGGACTT (reverse)
Nanog	GGGAACGCCTCATCAATGCC (forward) CAGAGGAAGGGCGAGGAGA (reverse)
c-Myc	CTGCATGAGGAGACACCGCC (forward) AGCCCGACTCCGACCTCTTG (reverse)
Cyc D2	GCGTGCAGAAGGACATCC (forward) CACTTTTGTTCCTCACAGA (reverse)
p21	GAGACCCCAGATAATTAAGGAC (forward) GAACAGGTCGGACATCAC (reverse)
AFP	GAAAAACTCTGGCGATGGGT (forward) CAGCAGCCTGAGAGTCCATA (reverse)
Sry (genomic DNA specific	CCCACTGCAGAAGGTTGT (forward) CCAGGAGGCACAGAGATT (reverse)
β-Actin	CGCCACCAGTTCCGCCATGGATG (forward) GGGAATACACCCGGGGAGCA (reverse)
GAPDH	ACGGCCGCATCTTCTTGTGCA (forward) CAGGCGCCCAATACGGCCAA (reverse)

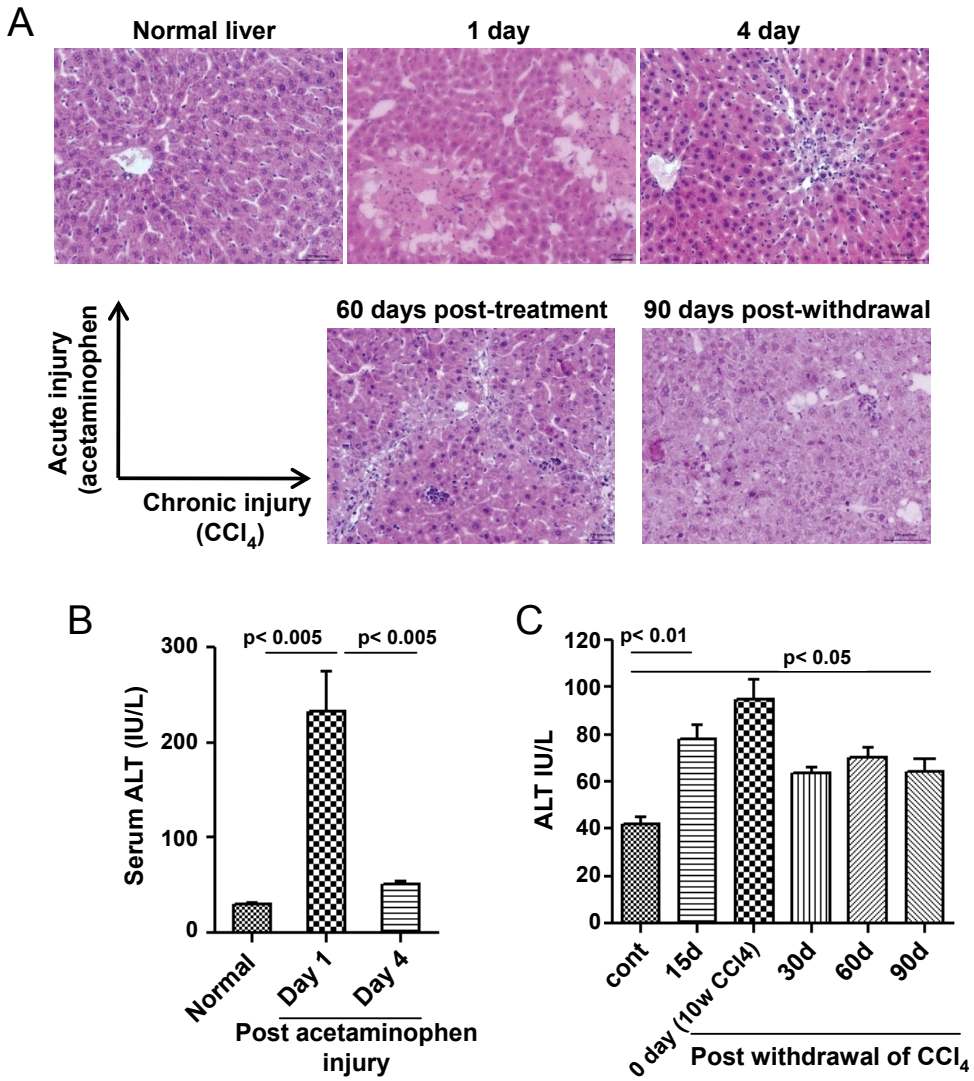

Figure 1: Acute and chronic liver injury model. (A) Top panel: Acute injury was inflicted by a single dose of acetaminophen in the mice. Centrilobular necrosis can be seen from the next day of administration, however mice recovered from injury associated pathological changes within 4 days. Bottom panel: Chronic injury was inflicted by multiple doses of CCl_4 in the mice. Liver fibrosis and steatosis can be seen after 8-10 weeks of injury. Some pathological improvement can be seen after 90 days of withdrawal of CCl_4 injection. Scale bar: 200 µm (200 ×). Number of mice = 3; (B) Serum ALT levels. Serum ALT level was increased within 1 day of acetaminophen administration, which reduces to normal level after 4 days (left bar diagram); (C) Serum ALT level did not fall to the normal level in case of chronic injury, even after 90 days of withdrawal of CCl_4 administration (right bar diagram). Number of mice in each group = 6.

bridges were seen (Figure 1A, bottom panel: left image) which was partially resolved on CCl_4 withdrawal. Macrovesicular hepatosteatosis was observed even post 90 days of CCl_4 withdrawal (Figure 1A, bottom panel, right image) with higher levels of serum ALT compared to healthy control (Figure 1C).

CD45 cell therapy improves liver fibrosis

CCl_4-induced liver fibrosis model was adopted to study the effect of donor derived $CD45^+$ cells in case of chronic injury. Each mouse was transplanted with 5 × 106 syngeneic GFP-expressing $CD45^+$ cells that were phenotypically highly heterogeneous, consisting of progenitors and committed hematopoietic cells (Supporting Figure 1A and Supporting Figure 1B) through intrasplenic route after 10 weeks of CCl_4 administration, and mice were sacrificed at different time periods to assess the resolution of fibrosis. Almost complete regression of fibrosis had occurred within 90 days of transplantation as evidenced in the picrosirius red and α-SMA stained liver sections, whereas natural regression in sham control (ShC) mice was much slower (Figure 2A). Interestingly, steady and significant drop of CPA by about 25% was observed in the Tx group within 15 days even under pro-fibrotic conditions, indicating that transplantation of CD45 cells resulted in improved clearance of collagen when compared with ShC (Figure 2B). Furthermore, transplantation of CD45 cells showed improving trend of liver function as sera ALT levels were declined as compared to ShC group (Supporting Figure 2). In contrast, no improvements of sera bilirubin and albumin levels were observed due to transplantation of cells, except for 3 months samples (Supporting Figure 2). According to these results the effect of the cell transplant seems to exert an acceleration of the natural process of restoration of the liver condition after withdrawal of CCl_4 dose.

Activated hepatic stellate cells (HpSCs) which secrete excess collagen in response to chronic injury, measured in terms of SMA-expressing cells (area) were also significantly ($p < 0.01$, 0.001) reduced in transplanted mice as compared with ShC mice, indicating that $CD45^+$ cells were either involved in deactivating the activated HpSCs or inducing their apoptosis or both (Figure 2A and Figure 2C).

As about 60% of donor cells were composed of monocytes/macrophages and neutrophils, we propose that enhanced recovery of liver from fibrosis was due to the effect of MMPs secreted by these cells. Tissue level gene expression analysis showed that except for MMP2, the expressions of MMP9, 12, 13 were significantly ($p < 0.05$, 0.01, $n = 2$ for each time point) increased post 7 and 15 days of CD45 transplantation when compared with corresponding ShC groups (Figure 3A).

To know the subset of $CD45^+$ cells that was primarily responsible for regression of fibrosis, we divided transplant into two fractions: $CD45^+CD11b^-Ly6g^-$ (hematopoietic cells other than macrophages/monocytes and neutrophils) and $CD45^+11b^+Ly6g^{+/-}$ (macrophages/monocytes and neutrophils). The control group received $CD45^+$ cells, like earlier experiments. The results showed both these subsets reduced

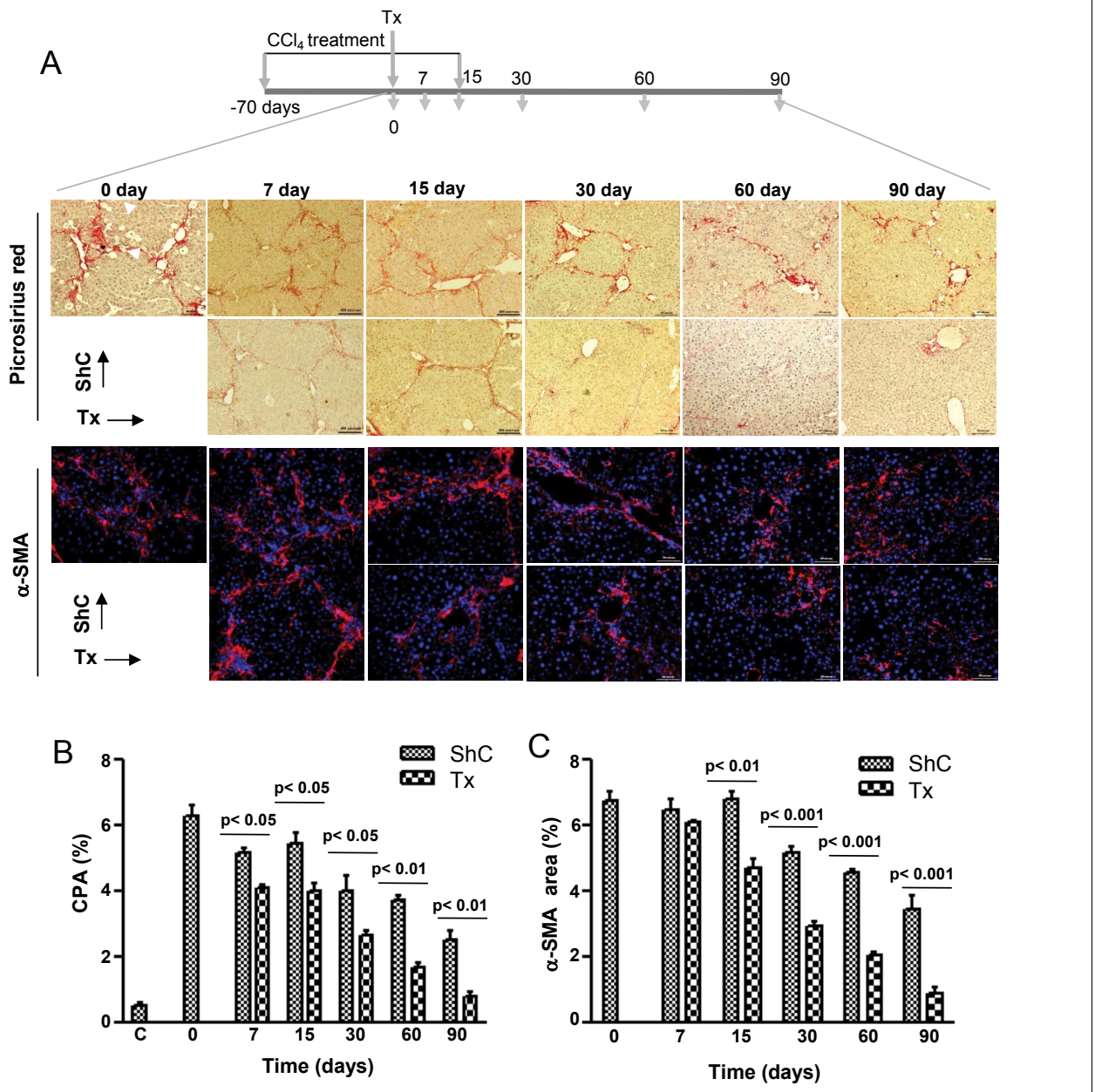

Figure 2: Therapeutic effect of CD45 cells on fibrosis. (A) Five million cells were transplanted in each mouse after 10 weeks of CCl_4 treatment. Thereafter, profibrotic condition was maintained for 15 days by injecting CCl_4. Liver sections at different time intervals, as shown in the figure, were stained with picrosirius red and α-SMA. The representative micrographs are shown. Scale bars: 400 μm (100 ×), 200 μm (200 ×); (B) Collagen proportionate area. Collagen synthesis in transplantation group was significantly reduced as compared to sham control; (C) α-SMA area. Expression of α-SMA in transplantation group was reduced as compared to ShC. In B & C, 30 non-overlapping fields from multiple liver sections were taken for area calculation. Number of mice in each time point = 6. ShC: Sham control, Tx: Transplantation, C: Healthy control.

fibrosis (CPA) when compared with the control (6.24 ± 0.18%, n = 3), but it was significant only in case of $CD45^+11b^+Ly6g^{+/-}$ fraction (3.7 ± 0.07%, n = 3), as shown in figure 3B. Comparing between the subsets, $CD45^+11b^+Ly6g^{+/-}$ cells were found to be significantly ($p < 0.01$) more fibrolytic.

Another interesting observation was a significant reduction of apoptosis in both hepatocytes and non-parenchymal cells due to transplantation of CD45 cells. In pro-fibrogenic condition, the transplantation of CD45 cells led to significant decline of $TUNEL^+$ hepatocytes as compared with ShC mice (17.69 ± 3.43% versus 40.0 ± 3.29% per 600 × field, $p < 0.05$, n = 2) (Figure 4). Despite significant recovery apoptotic cells were present in Tx group, this was possible due to the effect of CCl_4 treatment as it was discontinued just 3 days prior to this analysis.

BM-derived stem/progenitor cells are involved in liver regeneration

To examine whether BM cells have any role in liver regeneration, we transplanted Lin^- cells in acute liver injured mice, whereas the chronic liver injured mice received $CD45^+$ cells. The number of cells transplanted and the route of transplantation in these models were different. The engraftment of donor cells and their phenotype was determined by immuno-histochemical analysis of the liver sections (Figure 5A, image). Morphometric analyses of the images (200 × magnification) in 30 different fields of liver sections (each mouse) after 3 months of transplantation in acute and chronic injured livers showed 5.6 ± 0.4% (n = 3) and 17.5 ± 0.7% (n = 3) of cells were GFP^+ Alb^+, respectively (Figure 5A, bar diagram). The presence of donor-derived hepatocytes after 7 and 15 days of transplantation in pro-fibrogenic condition are shown in Supporting Figure 3. The presence of BM-derived hepatocytes was further confirmed by co-staining tissue sections of acute liver injury model with eGFP and HNF4α antibodies (Figure 5B).

To find out whether CD45 cells transplantation led to activation of HPCs, we analyzed liver sections after 7 days of transplantation. Interestingly, ductular reaction was found to be relatively high in Tx group as EpCAM/CK-19 expressing cells were detected, but it was not significantly higher than ShC group (Figure 5C).

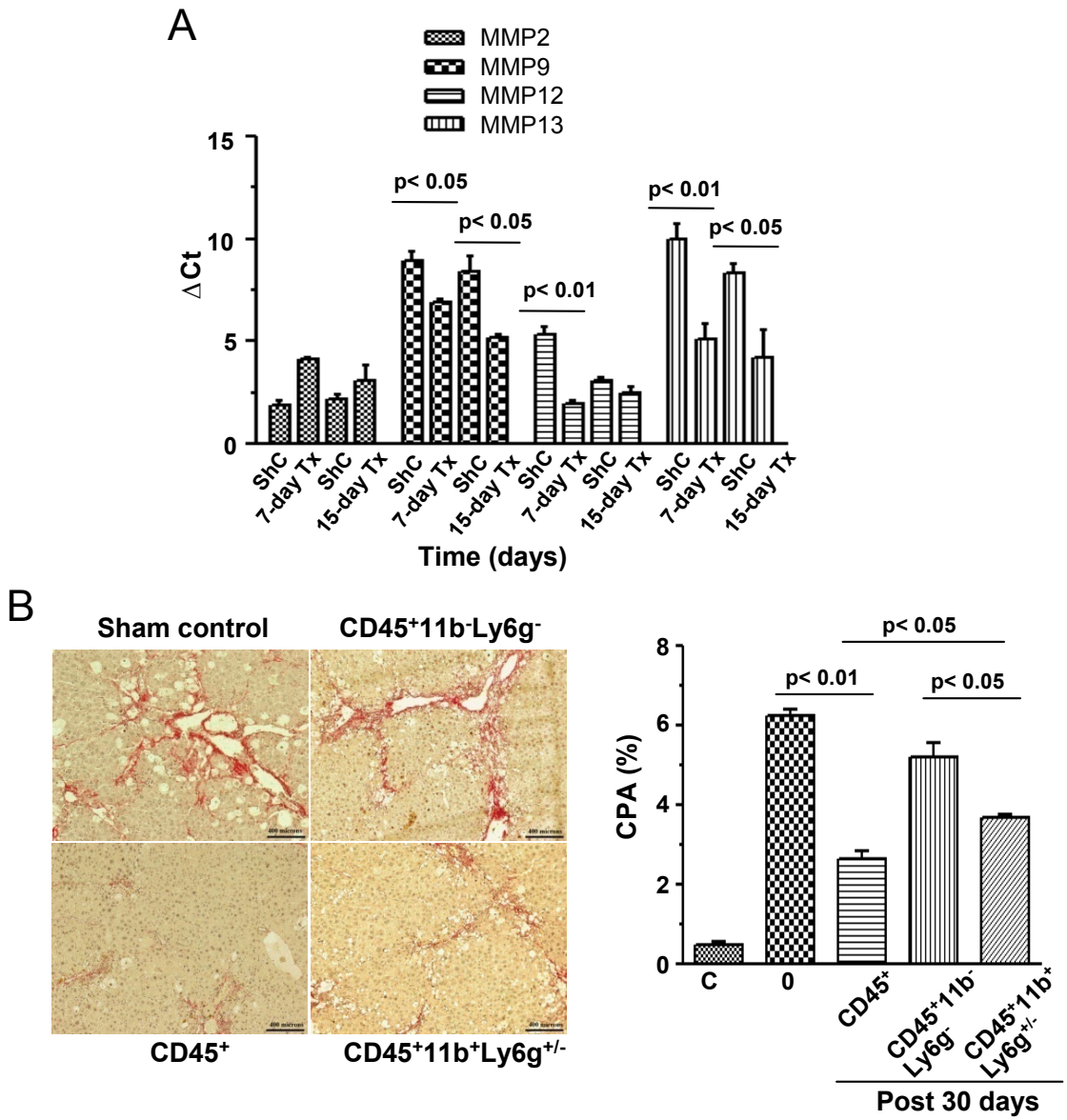

Figure 3: Tissue level expression of MMPs and effect of fibrolytic cells of CPA. (A) Liver tissue samples were analyzed after 7 and 15 days of transplantation for the expression of MMP-2,9,12,13 by quantitative RT-PCR. Gene expressions of both time points were compared with respective ShC samples. Number of mice in each time point = 3; (B) Five, three and two million CD45$^+$, CD45$^+$CD11b$^+$Ly6g$^{+/-}$, CD45$^+$CD11b$^-$Ly6g$^-$ cells, respectively were transplanted in each mouse of three groups after 10 weeks of CCl_4 treatment. Liver sections after 30 days of transplantation were stained with picrosirus red, the representative micrographs are shown. Collagen proportionate areas were determined by using Image J software. Number of mice in each time point = 3. Scale bars: 200 μm (200 ×). C: Healthy control.

Molecular analysis of donor-derived hepatocytes

During lineage conversion to hepatic phenotype, partial nuclear reprogramming of BM cells is expected to occur. Real time RT-PCR analysis of BM-derived hepatocytes showed that pan-hematopoietic (*CD45*) and stem cell antigen (*Sca-1*) genes were completely silenced, whereas expression of transcription factor *Gata2* was significantly down regulated in BM-derived hepatocytes (Figure 6A).

Donor-derived hepatic cells in acute injury model did not express stemness genes such as *Oct4*, *Sox2* and *Nanog* (Figure 6B). To study oncogenic transformation of the cells, we then conducted analyses of cell cycle and hepatocellular carcinoma (HCC) marker genes. The expression of *c-Myc* was marginally increased in these cells as compared to primary hepatocytes, whereas *Cyclin D2* and *p21* expressions were comparable (Figure 6C). Interestingly, HCC marker α-fetoprotein was not expressed in these cells (Figure 6C). Similar trend of gene expressions (tissue level) were also observed in case of chronic liver injury model (Supporting Figure 4A and Supporting Figure 4B). Above preliminary results indicate that nuclear reprogramming of BM-derived cells did not led to oncogenic transformation.

To investigate X,Y chromosomal status in BM-derived hepatic cells, an absolute quantification of Y chromosome marker *Sry* gene in recipient and donor-derived hepatocytes was conducted. The presence of Y-chromosome in GFP$^+$ cells fractions obtained in acute and chronic injury models were 1.85 ± 0.86% and 1.53 ± 0.85%, respectively (Figure 6D & Figure 6E). These results were supported by X,Y chromosome FISH analysis, confirming that the Y-chromosome in GFP$^+$ cells were under 6% (Figure 6F and Figure 6G). Low percentage of XY-chromosome bearing BM-derived hepatic cells in livers of both damaged models indicated that the fusion heterokaryons, if any, might have divided into host and donor-derived hepatocytes and maintained their sex chromosomal status.

Discussion

BM cell therapy has been found to be a promising treatment option for many liver diseases. Earlier reports suggested that under strong selection pressure, as in case of Fah$^{-/-}$ model, BM-derived hepatocytes, a putative product of fusion heterokaryons, can rapidly proliferate and replace the damaged/mutated host cells [7]. Heterokaryons are fairly unstable, during reductive division the abnormal chromosomal segregation may lead to neoplasia [20]. In this study, using acute and chronic liver injury models we have shown the presence of BM-

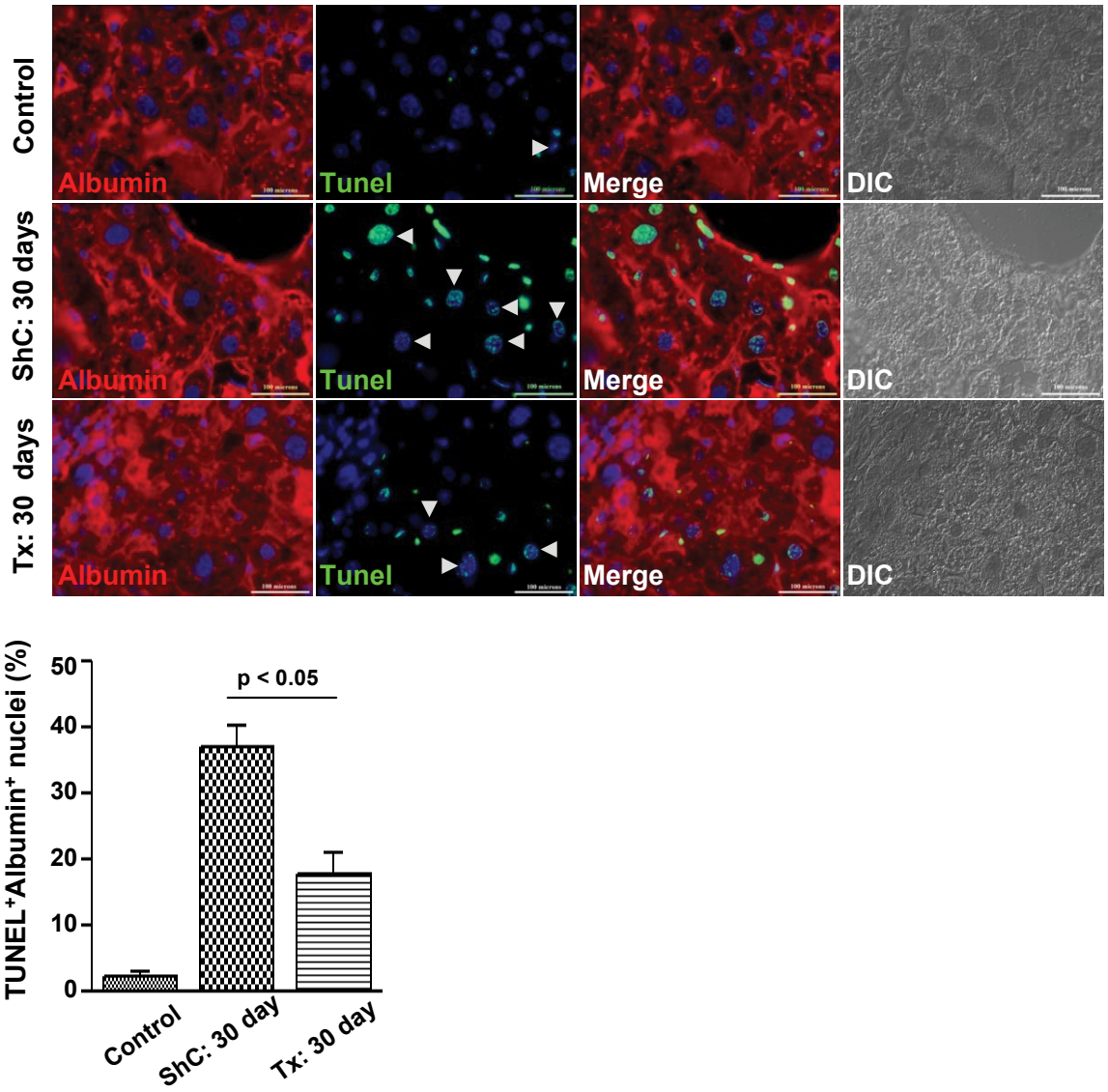

Figure 4: Effect of CD45 cell transplantation on apoptosis of hepatocytes. After 30 days of transplantation, the liver sections of ShC and Tx groups of mice were stained with albumin and then subjected to TUNEL reaction. TUNEL positive cells were reduced in Tx group as compared with ShC group. Scale bars: 100 μm (600 ×). Number of mice each group = 3.

derived hepatocytes till the end of the experiments. Interestingly, these neo hepatocytes present in host liver were found free from many genes associated with neoplasia.

The purpose of using two different preparations of cells in acute and chronic injury model was that liver fibrosis prevails in the later case. Our earlier report showed $CD45^+$ BM cells have better anti-fibrotic effects than mesenchymal stem cells [21]. Since monocytes/ macrophages and neutrophils have distinct roles in resolution of fibrosis through the secretion of MMP-9 and 13 [22,23], we transplanted $CD45^+$ cells, which was composed of about 55% $CD11b^+$ and $CD11b^+Ly6g^+$ cells. On the other hand, the acute injured mice were transplanted with only stem/progenitor cells. In fibrotic liver, the activated hepatic stellate cells (aHpSCs) deposit excessive collagen, which was not completely degraded by the endogenous MMPs of the mobilized BM cells and resident Kuffper cells (KCs). In transplanted mice, a steady drop in remnant collagen levels suggested a corrective role of $CD45^+$ cells by secreting adequate amount of MMP-9 and 13. The role of macrophages/monocytes in regression of fibrosis was proved by transplanting only $CD45^+CD11b^+Ly6g^{+/-}$ cells, where we had expected complete regression as seen in case of CD45 cells, however it was much lower. This suggested that other fraction of CD45 cells ($CD45^+CD11b^-Ly6g^-$) additively contributes to the recovery of liver from fibrosis. The gradual decline of aHpSCs in Tx mice was probably due to apoptotic stimuli from the activated macrophages and KCs [24] or natural deactivation process mediated by progenitor cells present in $CD45^+CD11b^-Ly6g^-$ fraction.

Between the two models examined, chronic liver injury showed 3-fold more BM-derived hepatocytes than the acute injury model. In chronic injury model, intrasplenic transplantation allowed direct cell delivery to the liver and subsequent engraftment of major fraction of the competent cells. During chronic injury, liver was repeatedly injured with CCl_4, which lead to continuous degeneration and regeneration allowing slow but steady incorporation of BM-derived cells during the regeneration process, so a higher level of chimerism was detected. On the other hand, systemic route was followed to deliver cells in case of acute injury model leading to wide distribution throughout the body and relatively less number of cells homing to the liver. Again, adult liver can regenerate at earliest on its' own as the mature hepatocytes can extensively proliferate [25]. Due to this brief regeneration period, the donor-derived cells may not play a major role in liver regeneration. Our earlier studies and the reports from other groups supported this moderate level of liver chimerism by BM cells in case of acute injury [26-28].

Down-regulation or silencing of hematopoietic genes in the recipient liver after phenotype change suggested partial nuclear programming [29]. Pluripotent genes (*Oct4*, *Sox2*, and *Nanog*) are generally expressed in embryonic stages of mammals; these are also shown to be expressed in carcinomas, including HepG2 cell line [30,31]. Lack of expressions of these genes in neo hepatocytes or in recipient tissue (chronic injury) suggested that nuclear reprogramming of BM cells in these present experimental models did not activate these genes. G1/S cyclins (cyclin

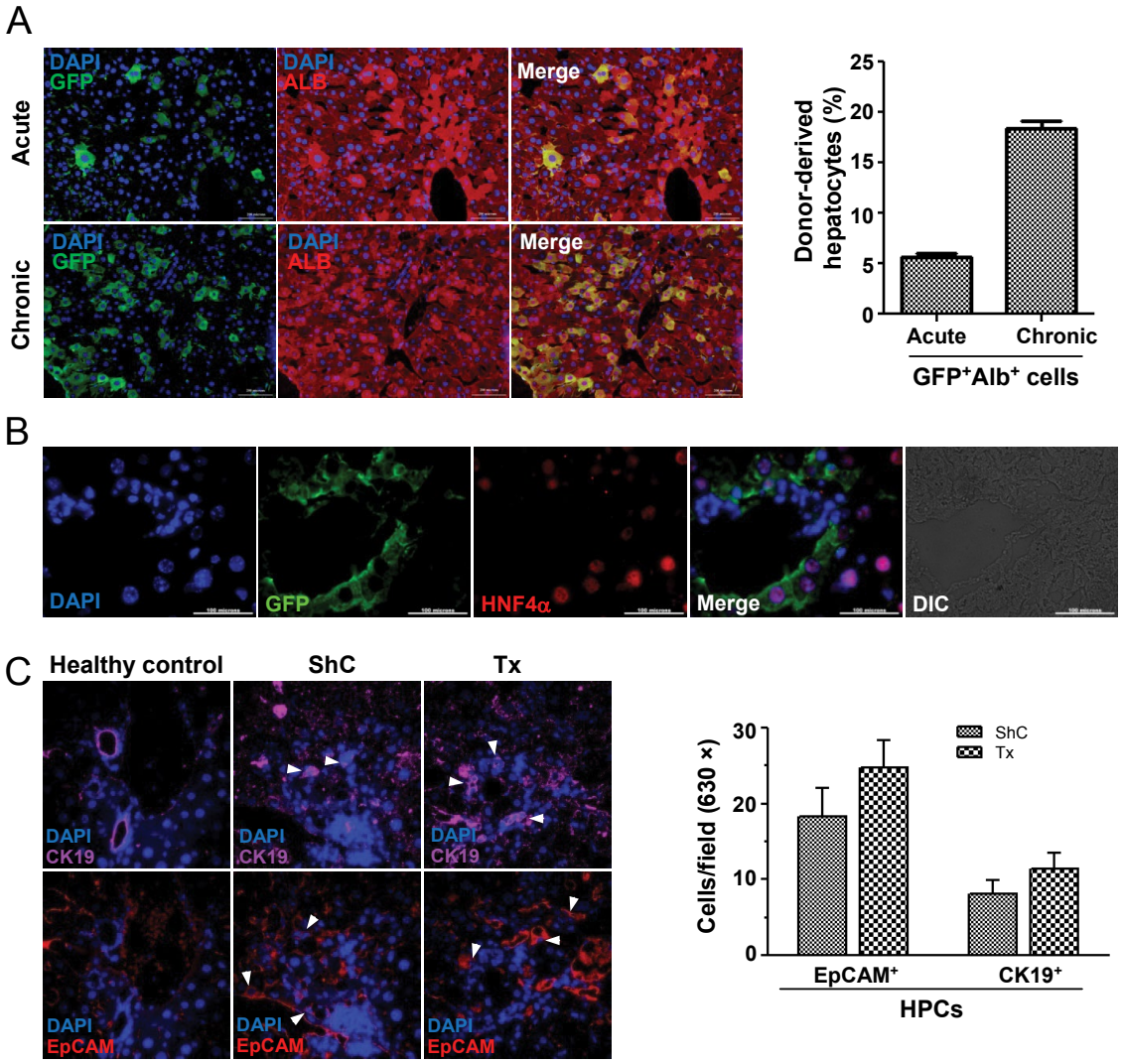

Figure 5: Phenotype conversion of engrafted BM cells. (A) Acute and chronic liver injured mice were transplanted with BM cells. After 90 days of transplantation, liver sections show BM-derived cells to express albumin (top panel: acute liver injury; bottom panel: chronic liver injury). Bar diagram showing the results of morphometric analysis (200 ×magnification), in which donor-cells expressed albumin in acute and chronic injured liver, respectively. Scale bar: 200 µm (200 ×). Number of mice = 3; (B) Liver sections of acute injured mice after 3 months of transplantation shows the expression of nuclear HNF-4α and GFP in donor-derived hepatocytes. Scale bar: 100 µm (600 ×) Number of mice = 3; (C) After 7 days of transplantation liver sections were individually stained for EpCAM or CK19 antigen. Representative images show ductular reaction. The bar diagram show EpCAM$^+$/CK19$^+$ cells per field, no significant differences in numbers of these cells were obtained between ShC and Tx group. Magnification: 600 ×; number of mice in each group = 2.

D2 and E2) were found to be negatively regulated by miR-26a, thereby control cell growth [32]. CDK inhibitor p21, a target of miR-106b and miR-93, was found to be over expressed in HCC [33]. Absence of p21 gene expression further suggests neoplastic transformation did not occur in BM-derived hepatocytes after partial reprogramming. c-Myc, a proto-oncogene, has been implicated as a regulator of hepatocyte proliferation and metabolic functions [34,35]. As an early gene, c-Myc expression has been reported to be induced following partial hepatectomy, and is a key factor in the transcriptional response leading to the progression of hepatocytes from G0/G1 to S phase [36]. Relatively high expression of c-Myc in BM-derived hepatocytes was probably due to their immaturity and proliferation status as compared to adult primary hepatocytes.

Heterotypic cell fusion between donor BM cells and host hepatocytes can generate either a synkaryon produced by the merging of nuclei or a binucleated heterokaryon in the absence of nuclear fusion. Irrespective of the partial nuclear reprogramming that might have occurred in one of the fusion partners (BM-derived hepatocytes), we could not detect numerous fused cells in eGFP$^+$ fraction of hepatocytes post 3 months of transplantation, as determined by the alternate methods. Even though BM-derived hepatocytes were formed due to cell fusion, we predict that the ploidy status in both cell types was restored due to a combination of cellular proliferation, fusion, and reductive division [37]. The other aspect of this study was that in spite of cell fusion that used to be the principle mechanism of phenotype conversion, we detected only a few donor-derived hepatocytes that possessed Y chromosome. This still puts forth the question as to the origin of the remaining BM derived hepatocytes. Overall, our study shows the significance of BM cell therapy in resolution of fibrosis and liver regeneration. Furthermore, the preliminary molecular analyses do not reveal any genetic changes in the BM-derived hepatocytes that may lead to neoplasia. In clinical translation, BM cell therapy would be an ideal approach to treat many liver diseases, which warrants detailed investigation.

Acknowledgement

The work was partly funded by Department of Biotechnology, Government of India under the Centre for Molecular Medicine programme.

Ethical Statement

All experiments were conducted as per procedures approved by the Institutional Animal Ethics Committee at the National Institute of Immunology, New Delhi, India.

Author's Contribution

Prakash Baligar and Veena Kochat have equal contributions.

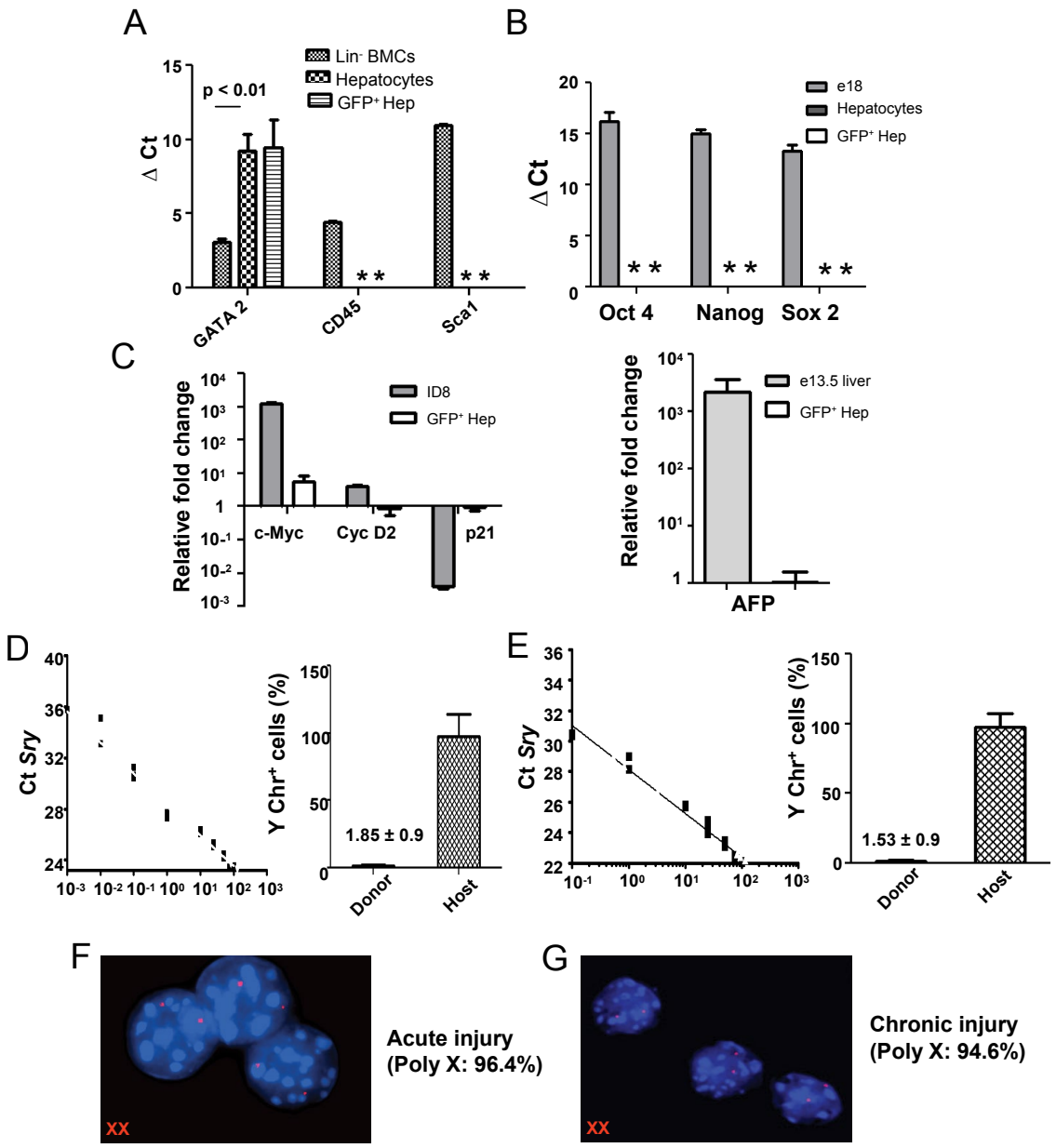

Figure 6: Expression of various genes in post nuclear reprogrammed BM-derived hepatocytes. (A) Expression of hematopoietic markers in donor-derived cells. Real time RT-PCR analysis shows loss or down-regulation of *GATA2*, *CD45* and *Sca1* genes; (B) Pluripotent and tumor gene expression. In above experiments, donor derived cells were analyzed with respect to the expression of *Sox2*, *Oct4*, *Nanog* by qPCR. As controls, fetal and normal adult hepatocytes were used; (C) Quantitative RT-PCR analyses of cell cycle and HCC genes. Three months post-transplanted samples showed that donor-derived hepatic cells were no longer in proliferative state. ID8 tumor cell line was used as positive control and values were normalized with respect to host hepatocytes. Expression of *AFP* gene in fetal liver tissue and in BM-derived hepatocytes. *AFP* did not express in BM-derived hepatocytes. As controls, fetal and normal adult hepatocytes were used; (D & E) Quantitative PCR analyses of *Sry* gene in genomic DNA of sorted cells. The Ct values of the unknown samples (red triangle); the donor and host hepatocytes (in both acute and chronic liver injury models) were fit in the standard curve and the presence of *Sry* gene was determined. Bar diagrams suggest that less than 2% of the donor-derived cells contained *Sry* gene. '*' indicated no Ct values; (F & G) X,Y FISH analysis of sorted cells. The representative images show donor derived hepatic cells consist of only XX chromosomes. Poly X means 2X, 4X and 6X cells. Analyses were based on 3 sets of samples.

References

1. Alvarez-Dolado M, Pardal R, Garcia-Verdugo JM, Fike JR, Lee HO, et al. (2003) Fusion of bone-marrow-derived cells with Purkinje neurons, cardiomyocytes and hepatocytes. Nature 425: 968-973.
2. Danet GH, Luongo JL, Butler G, Lu MM, Tenner AJ, et al. (2002) C1qRp defines a new human stem cell population with hematopoietic and hepatic potential. Proc Natl Acad Sci U S A 99: 10441-10445.
3. Kanazawa Y, Verma IM (2003) Little evidence of bone marrow-derived hepatocytes in the replacement of injured liver. Proc Natl Acad Sci U S A 100 Suppl 1: 11850-11853.
4. Theise ND, Badve S, Saxena R, Henegariu O, Sell S, et al. (2000) Derivation of hepatocytes from bone marrow cells in mice after radiation-induced myeloablation. Hepatology 31: 235-240.
5. Wagers AJ, Sherwood RI, Christensen JL, Weissman IL (2002) Little evidence for developmental plasticity of adult hematopoietic stem cells. Science 297: 2256-2259.
6. Lagasse E, Connors H, Al-Dhalimy M, Reitsma M, Dohse M, et al. (2000) Purified hematopoietic stem cells can differentiate into hepatocytes *in vivo*. Nat Med 6: 1229-1234.
7. Wang X, Willenbring H, Akkari Y, Torimaru Y, Foster M, et al. (2003) Cell fusion is the principal source of bone-marrow-derived hepatocytes. Nature 422: 897-901.
8. Cantz T, Sharma AD, Jochheim-Richter A, Arseniev L, Klein C, et al. (2004) Reevaluation of bone marrow-derived cells as a source for hepatocyte regeneration. Cell Transplant 13: 659-666.
9. Willenbring H, Bailey AS, Foster M, Akkari Y, Dorrell C, et al. (2004) Myelomonocytic cells are sufficient for therapeutic cell fusion in liver. Nat Med 10: 744-748.
10. Kochat V, Baligar P, Maiwall R, Mukhopadhyay A (2014) Bone marrow stem-cell therapy for genetic and chronic liver diseases. Hepatol Int 8: 166-178.
11. Mukhopadhyay A (2013) Perspective on liver regeneration by bone marrow-derived stem cells-a scientific realization or a paradox. Cytotherapy 15: 881-892.

12. Usunier B, Benderitter M, Tamarat R, Chapel A (2014) Management of fibrosis: the mesenchymal stromal cells breakthrough. Stem Cells Int 2014: 340257.

13. El-Ansary M, Mogawer S, Abdel-Aziz I, Abdel-Hamid S (2010) Phase I trial: Mesenchymal stem cells transplantation in end stage liver disease. J Am Sci 6: 135-144.

14. Kharaziha P, Hellstrom PM, Noorinayer B, Farzaneh F, Aghajani K, et al. (2009) Improvement of liver function in liver cirrhosis patients after autologous mesenchymal stem cell injection: a phase I-II clinical trial. Eur J Gastroenterol Hepatol 21: 1199-1205.

15. Muraca M, Ferraresso C, Vilei MT, Granato A, Quarta M, et al. (2007) Liver repopulation with bone marrow derived cells improves the metabolic disorder in the Gunn rat. Gut 56: 1725-1735.

16. Saito T, Okumoto K, Haga H, Nishise Y, Ishii R, et al. (2011) Potential therapeutic application of intravenous autologous bone marrow infusion in patients with alcoholic liver cirrhosis. Stem Cells Dev 20: 1503-1510.

17. Salama H, Zekri AR, Zern M, Bahnassy A, Loutfy S, et al. (2010) Autologous hematopoietic stem cell transplantation in 48 patients with end-stage chronic liver diseases. Cell Transplant 19: 1475-1486.

18. Terai S, Tanimoto H, Maeda M, Zaitsu J, Hisanaga T, et al. (2012) Timeline for development of autologous bone marrow infusion (ABMi) therapy and perspective for future stem cell therapy. J Gastroenterol 47: 491-497.

19. Bird TG, Lu WY, Boulter L, Gordon-Keylock S, Ridgway RA, et al. (2013) Bone marrow injection stimulates hepatic ductular reactions in the absence of injury via macrophages-mediated TWEAK signaling. Proc Natl Acad Sci USA 110: 6542-6547.

20. Jallepalli PV, Lengauer C (2001) Chromosome segregation and cancer: cutting through the mystery. Nat Rev Cancer 1: 109-117.

21. Baligar P, Mukherjee S, Kochat V, Rastogi A, Mukhopadhyay A (2015) Molecular and cellular functions distinguish superior therapeutic efficiency of bone marrow CD45 cells over mesenchymal stem cells in liver cirrhosis. Stem cells 34: 135-147.

22. Duffield JS, Forbes SJ, Constandinou CM, Clay S, Partolina M, et al. (2005) Selective depletion of macrophages reveals distinct, opposing roles during liver injury and repair. J Clin Invest 115: 56-65.

23. Yoshihara Y, Nakamura H, Obata K, Yamada H, Hayakawa T, et al. (2000) Matrix metalloproteinases and tissue inhibitors of metalloproteinases in synovial fluids from patients with rheumatoid arthritis or osteoarthritis. Ann Rheum Dis 59: 455-461.

24. Ramachandran P, Iredale JP (2012) Macrophages: central regulators of hepatic fibrogenesis and fibrosis resolution. J Hepatol 56: 1417-1419.

25. Overturf K, Al Dhalimy M, Ou CN, Finegold M, Grompe M (1997) Serial transplantation reveals the stem cell-like regenerative potential of adult mouse hepatocytes. Am J Pathol 151:1273-1280.

26. Jang YY, Collector MI, Baylin SB, Diehl AM, Sharkis SJ (2004) Hematopoietic stem cells convert into liver cells within days without fusion. Nat Cell Biol 6: 532-539.

27. Newsome PN, Johannessen I, Boyle S, Dalakas E, McAulay KA, et al. (2003) Human cord blood-derived cells can differentiate into hepatocytes in the mouse liver with no evidence of cellular fusion. Gastroenterology 124: 1891-1900.

28. Yadav N, Kanjirakkuzhiyil S, Kumar S, Jain M, Halder A, et al. (2009) The therapeutic effect of bone marrow-derived liver cells in the phenotypic correction of murine hemophilia A. Blood 114: 4552-4561.

29. Quintana-Bustamante O, Grueso E, Garcia-Escudero R, Arza E, Alvarez-Barrientos A, et al. (2012) Cell fusion reprogramming leads to a specific hepatic expression pattern during mouse bone marrow derived hepatocyte formation *In Vivo*. PLoS One 7: e33945.

30. Ling GQ, Chen DB, Wang BQ, Zhang LS (2012) Expression of the pluripotency markers Oct3/4, Nanog and Sox2 in human breast cancer cell lines. Oncol Lett 4: 1264-1268.

31. Amini S, Fathi F, Mobalegi J, Sofimajidpour H, Ghadimi T (2014) The expressions of stem cell markers: Oct4, Nanog, Sox, nucleostemin, Bmi, Zfx, Tcl, Tbx, Dppa4, and Esrrb in bladder, colon, and prostate cancer, and certain cancer cell lines. Anat Cell Biol 47: 1-11.

32. Zhu Y, Lu Y, Zhang Q, Liu JJ, Li TJ, et al. (2012) MicroRNA-26a/b and their host genes cooperate to inhibit the G1/S transition by activating the pRb protein. Nucleic Acids Res 40: 4615-4625.

33. Ivanovska I, Ball AS, Diaz RL, Magnus JF, Kibukawa M, et al. (2008) MicroRNAs in the miR-106b family regulate p21/CDKN1A and promote cell cycle progression. Mol Cell Biol 28: 2167-2174.

34. Collier JJ, Doan TT, Daniels MC, Schurr JR, Kolls JK, et al. (2003) c-Myc is required for the glucose-mediated induction of metabolic enzyme genes. J Biol Chem 278: 6588-6595.

35. Fausto N, Mead JE, Braun L, Thompson NL, Panzica M, et al. (1986) Proto-oncogene expression and growth factors during liver regeneration. Symp Fundam Cancer Res 39: 69-86.

36. Thompson NL, Mead JE, Braun L, Goyette M, Shank PR, et al. (1986) Sequential proto-oncogene expression during rat liver regeneration. Cancer Res 46: 3111-3117.

37. Duncan AW, Hickey RD, Paulk NK, Culberson AJ, Olson SB, et al. (2009) Ploidy reductions in murine fusion-derived hepatocytes. PLoS Genet 5: e1000385.

Supporting Methods

Animals: Six to eight-week-old male C57BL/6J and eGFP transgenic mice [C57BL/6-Tg(UBC-GFP)$_{30}$Scha/J] were used in this investigation. Mice were obtained from Jackson Laboratories (Bar Harbor, ME) and maintained in an experimental animal facility in our institute. Mice were kept in IVC and fed with autoclaved acidified water and irradiated food *ad libitum*.

Flow cytometry: BM CD45$^+$ cells were analyzed for different phenotypes, such as B220, CD3, CD34, CD11b, Ly6g-expressing cells using specific antibodies (BD Pharmingen) and FACS AriaIII (BD Bioscience, CA).

Isolation of hepatocytes and purity: Hepatocytes were isolated by two-stage perfusion method. Mice were anesthetized by intraperitoneal injection of ketamine (100 mg/kg) and xylazine (10 mg/kg), both were purchased from Helpro Health Product, Pune, India. In step I, the liver was perfused with 30 ml of Ca^{2+}/Mg^{2+} ion-free HBSS buffer containing 0.5 mM EGTA, 25 mM HEPES at 37 °C for 15 min, all were purchased from Sigma-Aldrich, St. Louise. In the step II, 30 ml of the same buffer, lacking EGTA, but containing 0.03% collagenase I (Sigma-Aldrich, St. Louise) and 5 mM $CaCl_2$ (Sigma-Aldrich, St. Louise) was used for perfusion. The liver capsule was incised and single-cell suspension was prepared in RPMI-1640 (Gibco, New York) containing 10% FBS (Biological Industries, Kibbutz Beit-Haemek, Israel) and separated through 100 µm cell strainer. Cell suspension was centrifuged at 50 *g* for 5 minutes to isolate hepatocytes from non-parenchyma cells, the pellet was washed two-times in the same medium. Donor and host hepatocytes were sorted on the basis of GFP expression. The sorted donor cells were then analyzed by immunocytochemistry on the basis of the expressions of albumin and GFP. Samples with > 96% cells expressing both GFP and albumin were considered as homogeneous preparation and used for the subsequent experiments.

Absolute quantification of *SRY* gene and XY chromosome FISH: We followed a sex-mismatched transplantation model where donor cells from female eGFP mice were transplanted into male non-eGFP mice. Absolute quantification of the *Sry* gene was carried out in GFP$^+$ and GFP$^-$ hepatocytes by real time qPCR (Stratagene MxPro 3000, Agilent Technologies, Santa Clara, CA) using SYBR green (Fermentas, Massachusetts) chemistry. Standards for *Sry* gene were prepared by mixing known numbers of female (XX) and male (XY) hepatocytes at different dilutions (100%, 75%, 50% 25%, 10%, 1%, 0.1%, 0.01%, 0.001% and 0% of Y chromosome containing cells) corresponding to the percentage fusion. Genomic DNA (gDNA) was isolated by kit (Fisher Scientific, Canada) from the standard cell mixtures and sorted GFP$^+$/GFP$^-$ hepatocytes. The same quantity of gDNA (100 ng) for each template was used for the PCR of *Sry* and *β-actin* genes. The Ct values of sorted samples were fit in the standard curve generated, and their percentage fusion was determined.

X,Y FISH was conducted on the basis on our earlier publication. In brief, fixed and denatured nuclei were reacted with whole-chromosome paint probes Poseidon™ RAB9B (XqF1) / WC Y mouse probe (Kreatech Diagnostics, Amsterdam, Netherlands) to detect X chromosome labeled with Platinum *Bright*™ 550 and Y chromosome labeled with Platinum *Bright*™ 495. The DAPI stained nuclei were visualized and scored using an upright Olympus BX51 fluorescence microscope (1000 ×). CytoVision™ and Genus™ imaging software (Applied Imaging, CA) were used to capture the images.

Gene expression: Total RNA was isolated from embryonic liver, ID8 cell line, primary hepatocytes (GFP$^-$) and sorted GFP$^+$ hepatocytes using TRIzol Reagent (Invitrogen, Carlsbad, CA) according to manufacturer's instructions, and cDNA was synthesized using High Capacity cDNA Reverse Transcription Kit (Applied Biosystems, CA). Real-time PCR was performed using SYBR green technology in a Stratagene Mx3000P QPCR System (Agilent, CA). The primers used for the PCR were synthesized from Sigma Life Science, Bangalore, India. The sequences of primers are provided in the table 1.

Apoptosis: Apoptotic cells were identified by TUNEL assay (Promega Corporation Madison, WI). In brief, paraffin embedded liver sections were stained for albumin. The TUNEL assay reagent was added on sections and incubated at 37°C for 1 h. Reaction was terminated with 2× SSC buffer, nuclei stained with DAPI and visualized under microscope.

Immunohistochemical analyses: Fixed cells and liver sections were stained with the respective antibodies. The sections or cells were observed under an Olympus fluorescence microscope and images were captured and acquired by DP70 digital camera (Model IX51, Olympus, Tokyo, Japan) using LCPlanFl 20 × and 60 × objectives by Image Pro software. The images were composed and edited in Photoshop 6.0 (Adobe). Antibodies used for IHC analysis were anti-mouse α-SMA (Imgenex, Bhubaneswar, India), anti-mouse eGFP (Clontech-Takara Bio Company, Kyoto, Japan), anti-mouse albumin (Bethyl, Montgomery, Texas), anti-mouse Ki67, anti-EpCAM (Abcam, Cambridge, UK), anti-HNF4α and anti-CK19 (Santa Cruz Biotechnology, Santa Cruz, CA). The secondary antibodies used were donkey anti-mouse Alexafluor 488, donkey anti-goat Alexafluor 594, donkey anti-rabbit Alexafluor 594, all of them were procured from Molecular Probes Inc, Eugene.

Liver function tests: Sera ALT, bilirubin and albumin levels were quantified by spectrophotometric methods, using commercially available kits (Transasia Bio-medicals Ltd, New Delhi, India).

1A

CONTROL

TEST

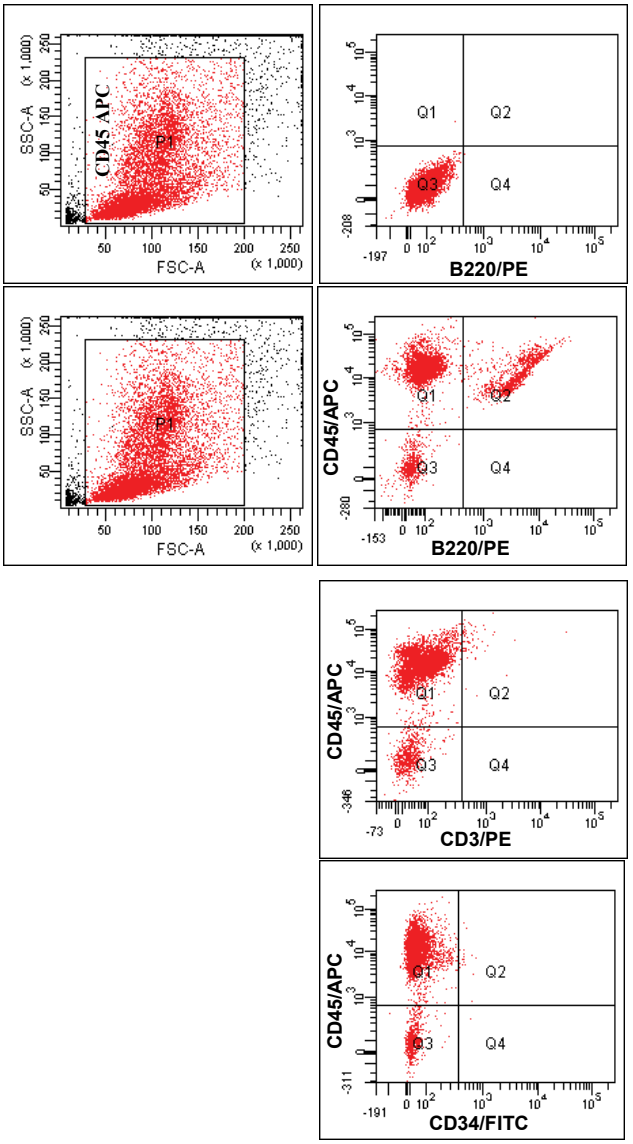

$B220^+$ cells: 28.1% of BM $CD45^+$ cells (mean of 3 samples)

$CD3^+$ cells: 1.44% of BM $CD45^+$ cells (mean of 3 samples)

$CD34^+$ cells: 0.44% of BM $CD45^+$ cells (mean of 3 samples)

1B

CONTROL

TEST

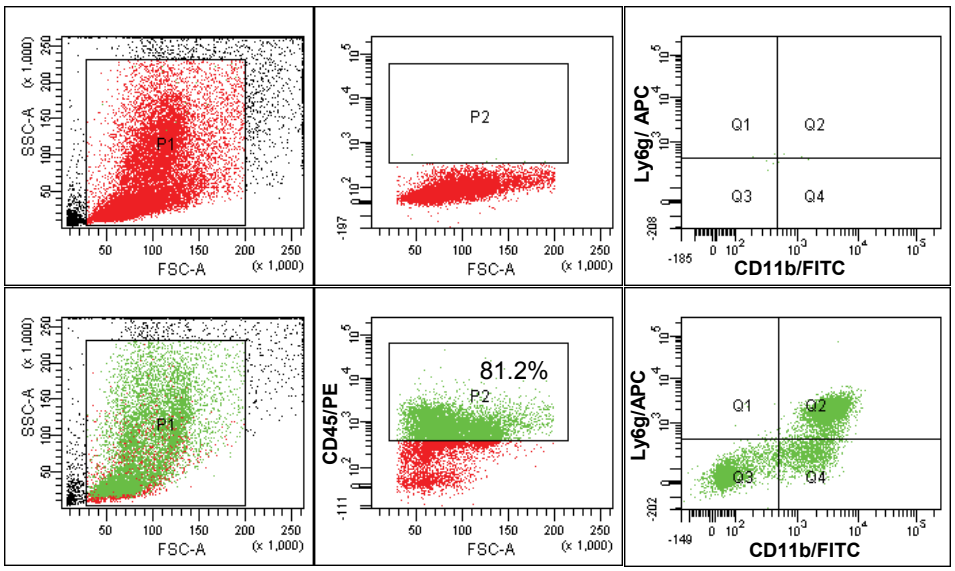

$CD45^+CD11b^+Ly6g^{+/-}$ cells: 55.15% of BM $CD45^+$ cells (mean of 3 samples)

Supporting Figure 1: Characterization of $CD45^+$ BM cells.

(A) Percentage of B cells ($B220^+$), T cells ($CD3^+$), progenitor cells ($CD34^+$) in transplanted $CD45^+$ cells were determined by flow cytometry; (B) Percentage of monocytes/ macrophages ($CD11b^+$) and neutrophils ($Ly6g^+$) in transplanted $CD45^+$ cells were also determined by flow cytometry. Number of mice = 3.

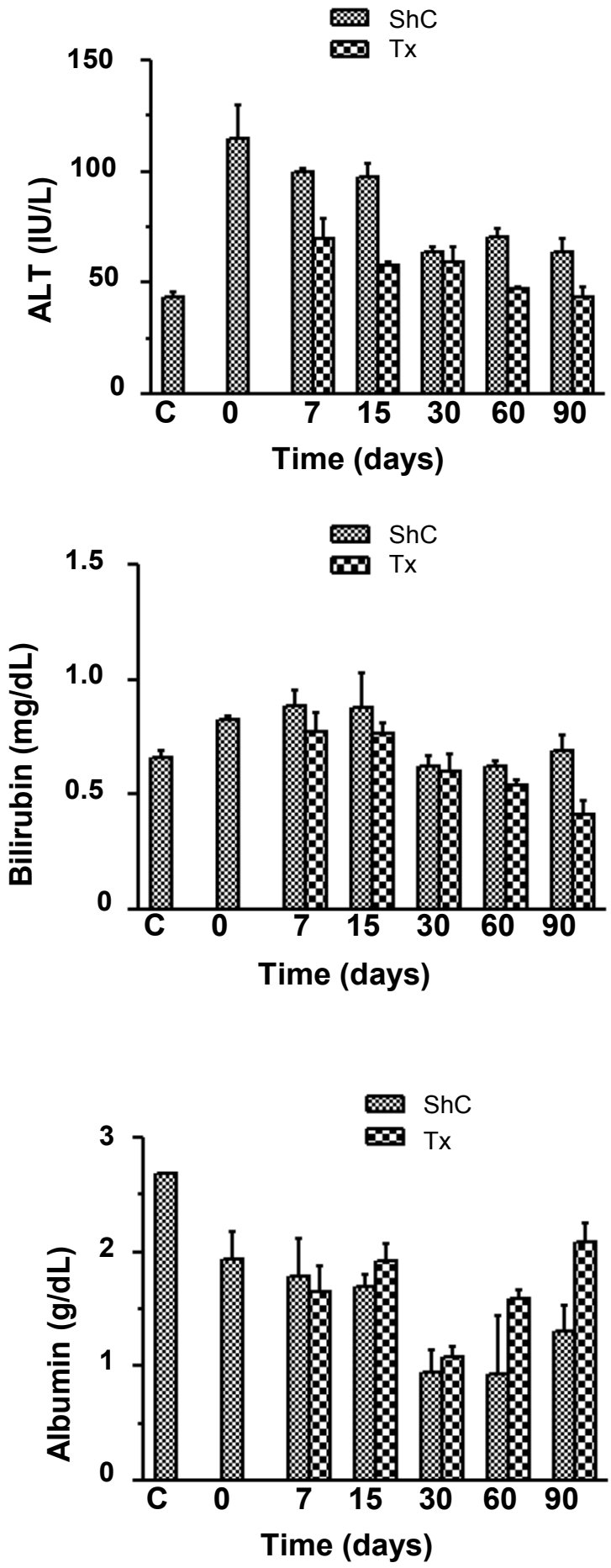

Supporting Figure 2: Analysis of liver functions in chronic liver injury after CD45⁺ cell transplantation.

Time course analysis of the improvement in liver functions after CD45⁺ transplantation in chronic liver injured mice (Tx) was done by determining the serum levels of ALT, bilirubin and albumin and compared with the levels in sham control (ShC) mice. Number of mice used for analysis in each time point = 3.

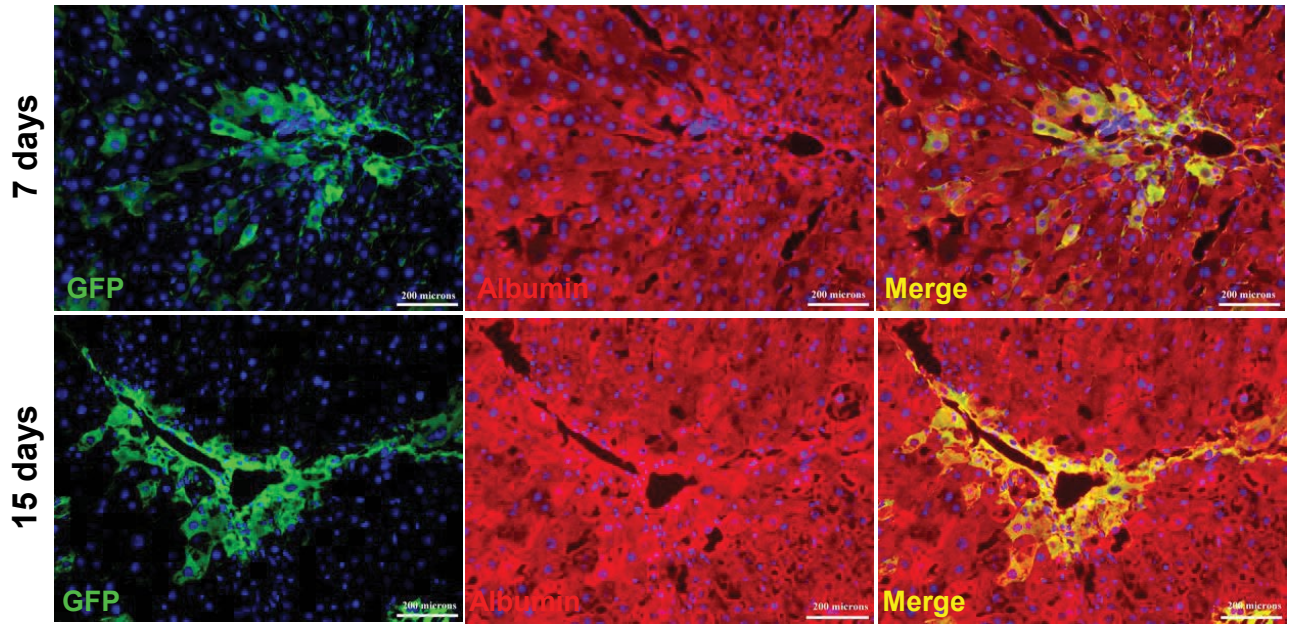

Supporting Figure 3: Liver regeneration in chronic liver injured mice by donor CD45⁺ cells.

Donor-derived hepatocytes expressing eGFP and albumin after 7 and 15 days of transplantation in pro-fibrogenic condition after CCl_4 induced chronic liver injury was analyzed by immunohistochemistry. Number of mice analyzed in each time point = 3.

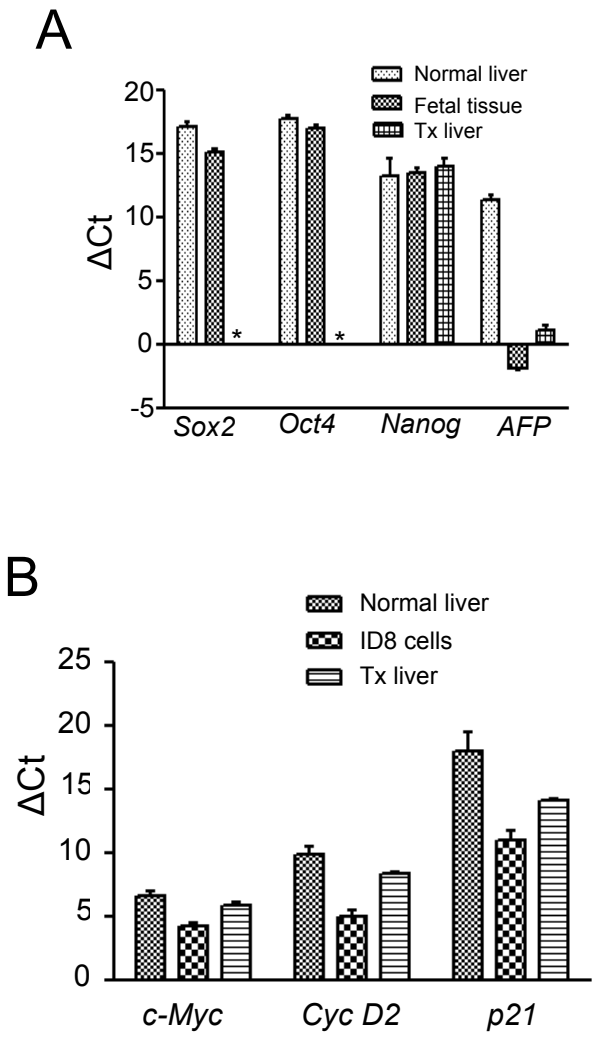

Supporting Figure 4: Analysis for the tumorigenic transformation of BM-derived hepatocytes in chronic injured liver tissue.

(A) Pluripotent (*Sox2*, *Oct4*, *Nanog*) and HCC related (AFP) gene expression in liver tissue of chronic liver injured mice after 3 months of CD45⁺ transplantation by qPCR. As controls, fetal tissue and normal adult hepatocytes were used. * denotes no Ct value; (B) Quantitative RT-PCR analyses of cell cycle genes in three months post-transplanted samples. ID8 tumor cell line was used as positive control. Number of mice in each group = 3.